Supplementary Material

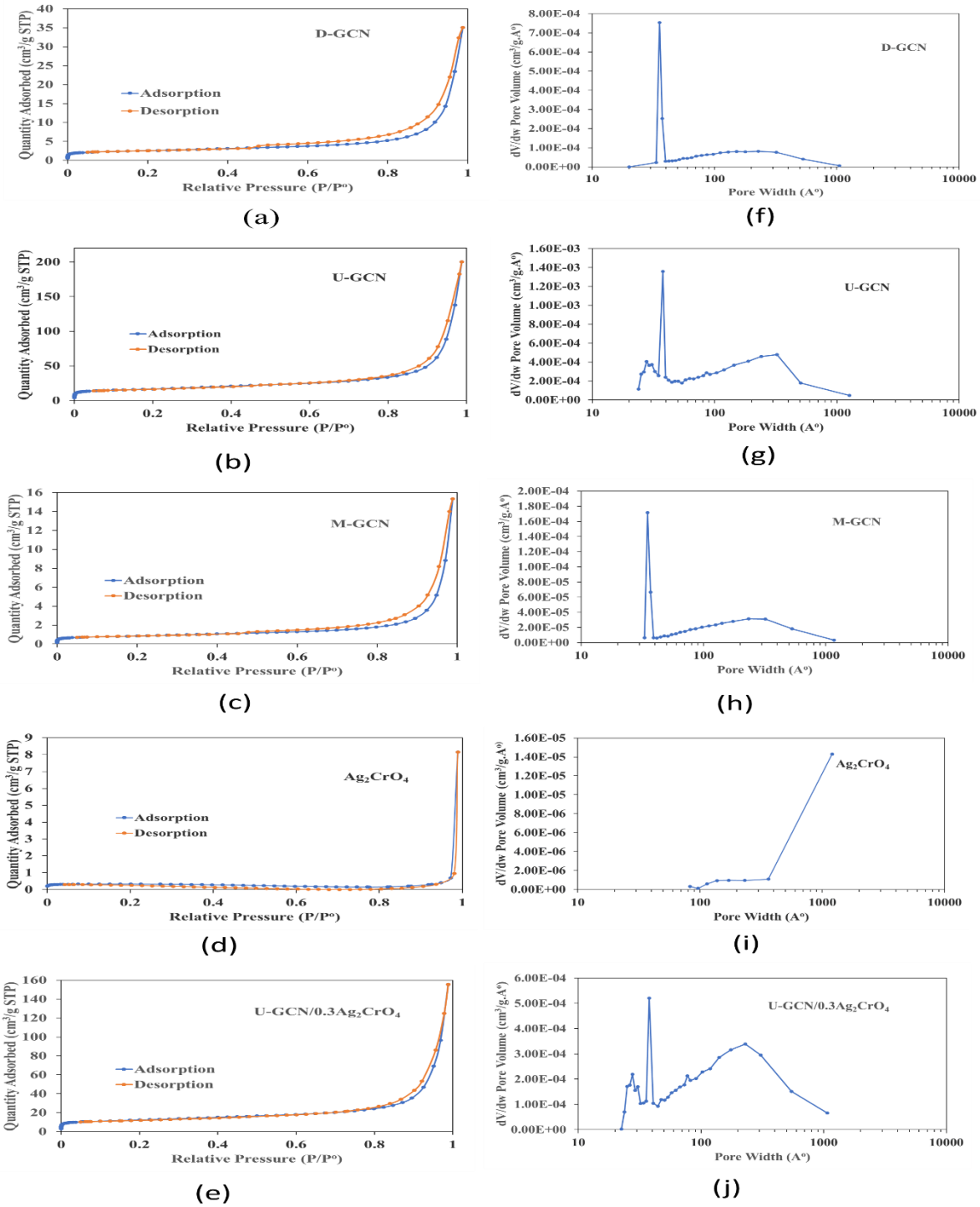

Figure S1. N_2 adsorption-desorption isotherms and their corresponding pore size distribution curves for the photocatalysts: D-GCN, U-GCN, M-GCN, Ag_2CrO_4, and U-GCN/0.3Ag_2CrO_4

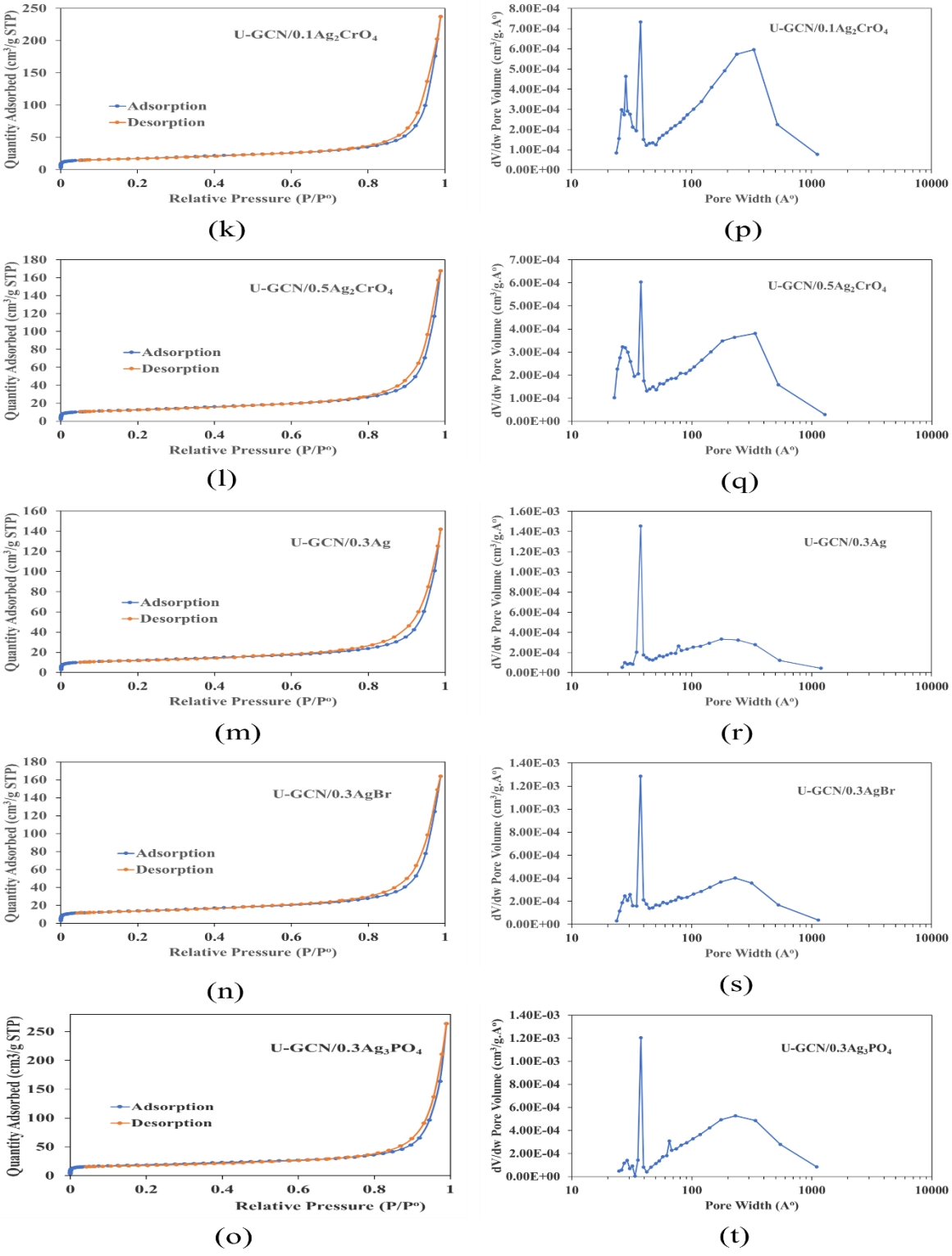

Figure S2. N_2 adsorption-desorption isotherms and their corresponding pore size distribution curves for the photocatalysts: U-GCN/0.1Ag_2CrO_4, U-GCN/0.5Ag_2CrO_4, U-GCN/0.3Ag, U-GCN/0.3AgBr, and U-GCN/0.3Ag_3PO_4

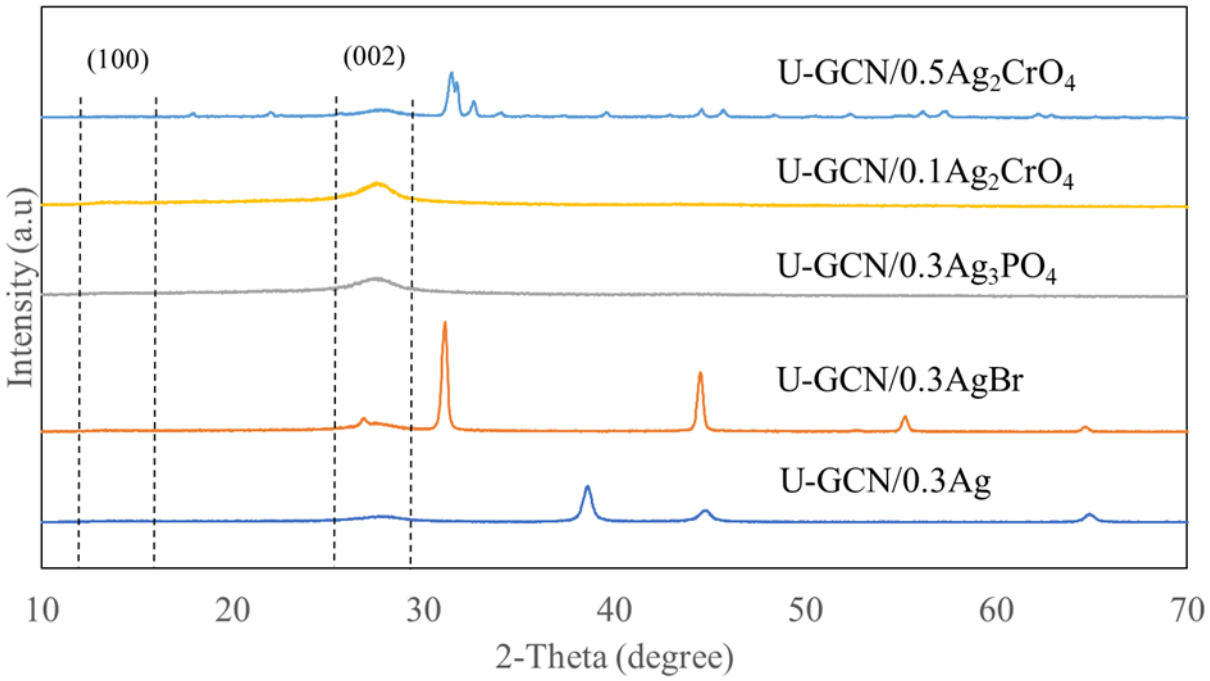

Figure S3. XRD patterns for the photocatalysts: U-GCN/silver-based composites and U-GCN/silver chromate composites

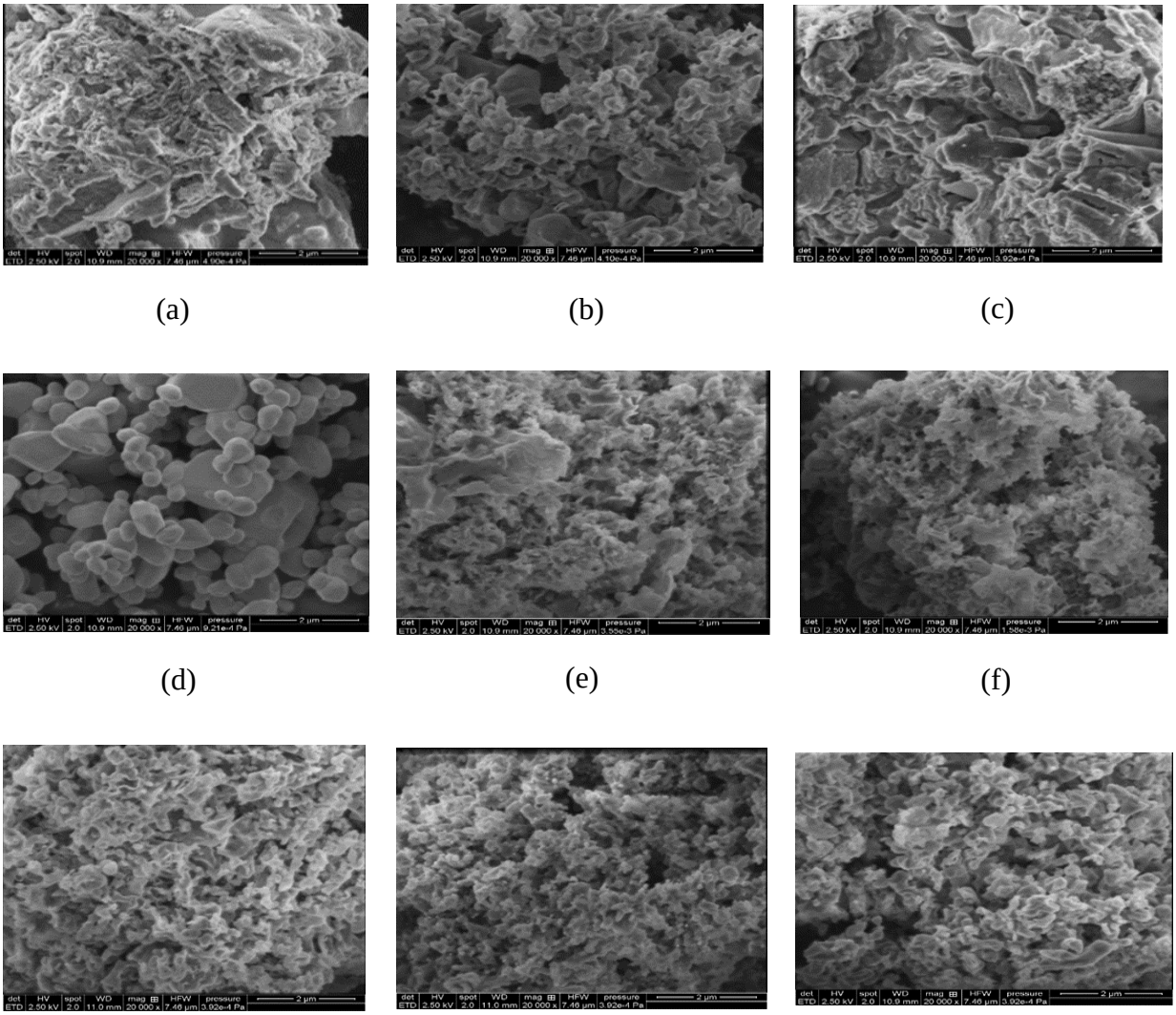

(a) (b) (c)

(d) (e) (f)

(g) (h) (i)

Figure S4. SEM images for the photocatalysts: (a) D-GCN, (b) U-GCN, (c) M-GCN, (d) Ag_2CrO_4, (e) U-GCN/0.1Ag_2CrO_4, (f) U-GCN/0.5Ag_2CrO_4, (g) U-GCN/0.3Ag, (h) U-GCN/0.3AgBr, and (i) U-GCN/0.3Ag_3PO_4

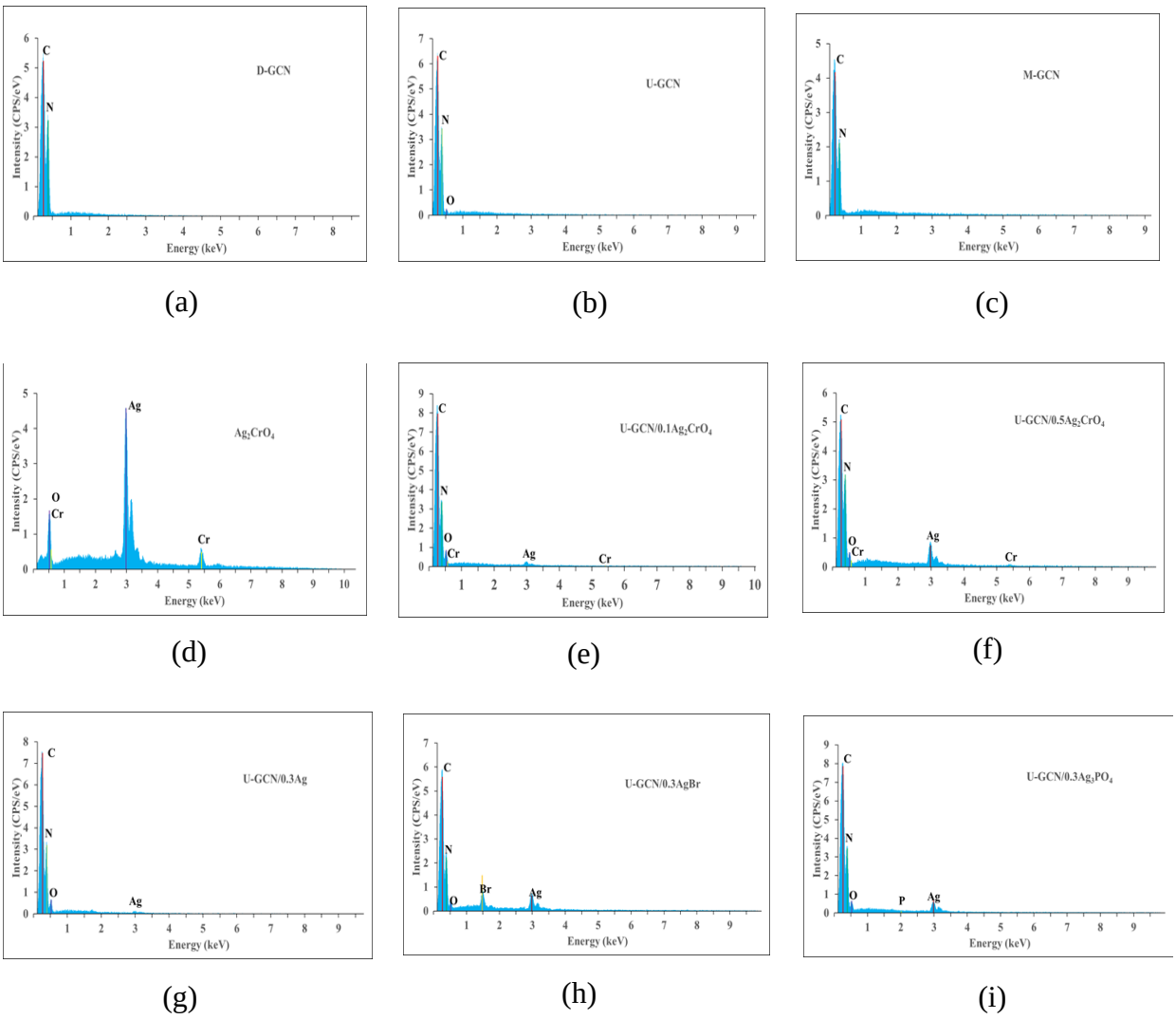

(a) (b) (c)

(d) (e) (f)

(g) (h) (i)

Figure S5. EDS images for the photocatalysts: (a) D-GCN, (b) U-GCN, (c) M-GCN, (d) Ag_2CrO_4, (e) U-GCN/0.1Ag_2CrO_4, (f) U-GCN/0.5Ag_2CrO_4, (g) U-GCN/0.3Ag, (h) U-GCN/0.3AgBr, and (i) U-GCN/0.3Ag_3PO_4

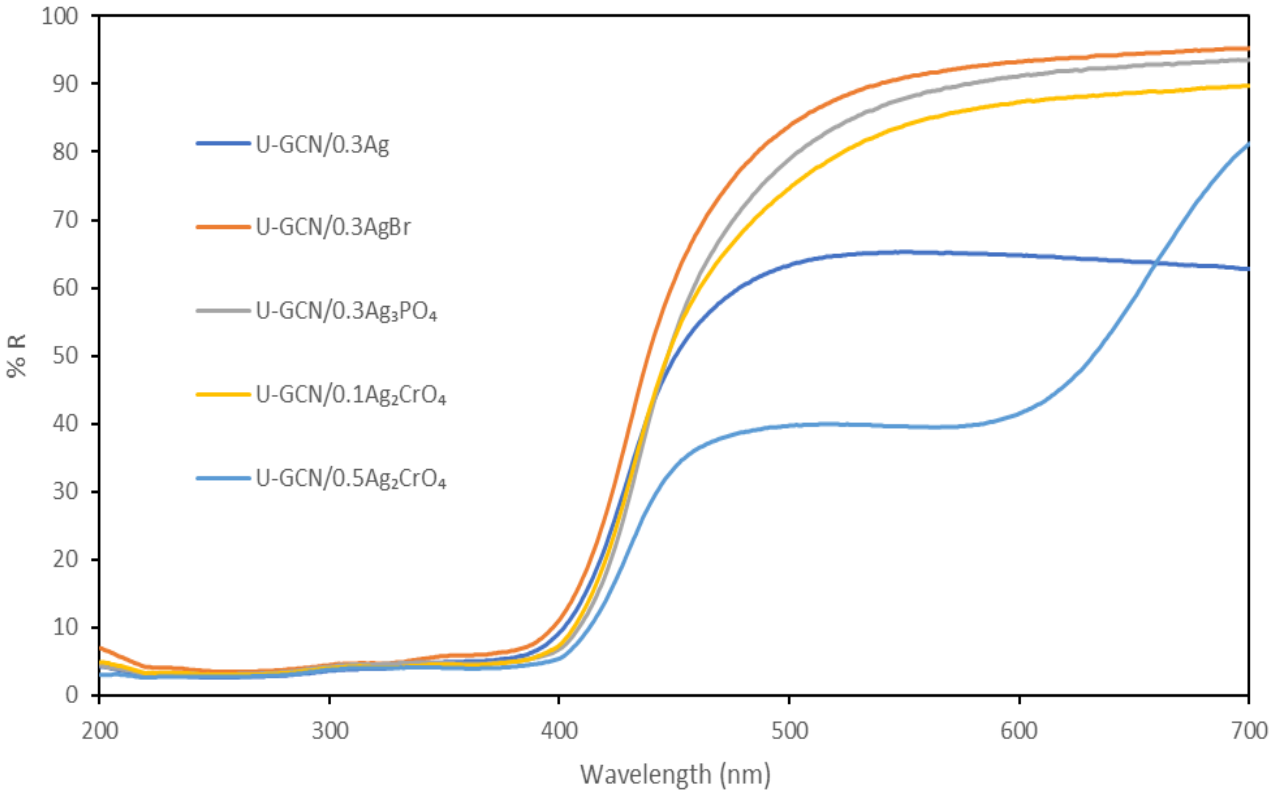

Figure S6. UV-Vis DRS for the photocatalysts: U-GCN/silver-based composites and U-GCN/silver chromate composites

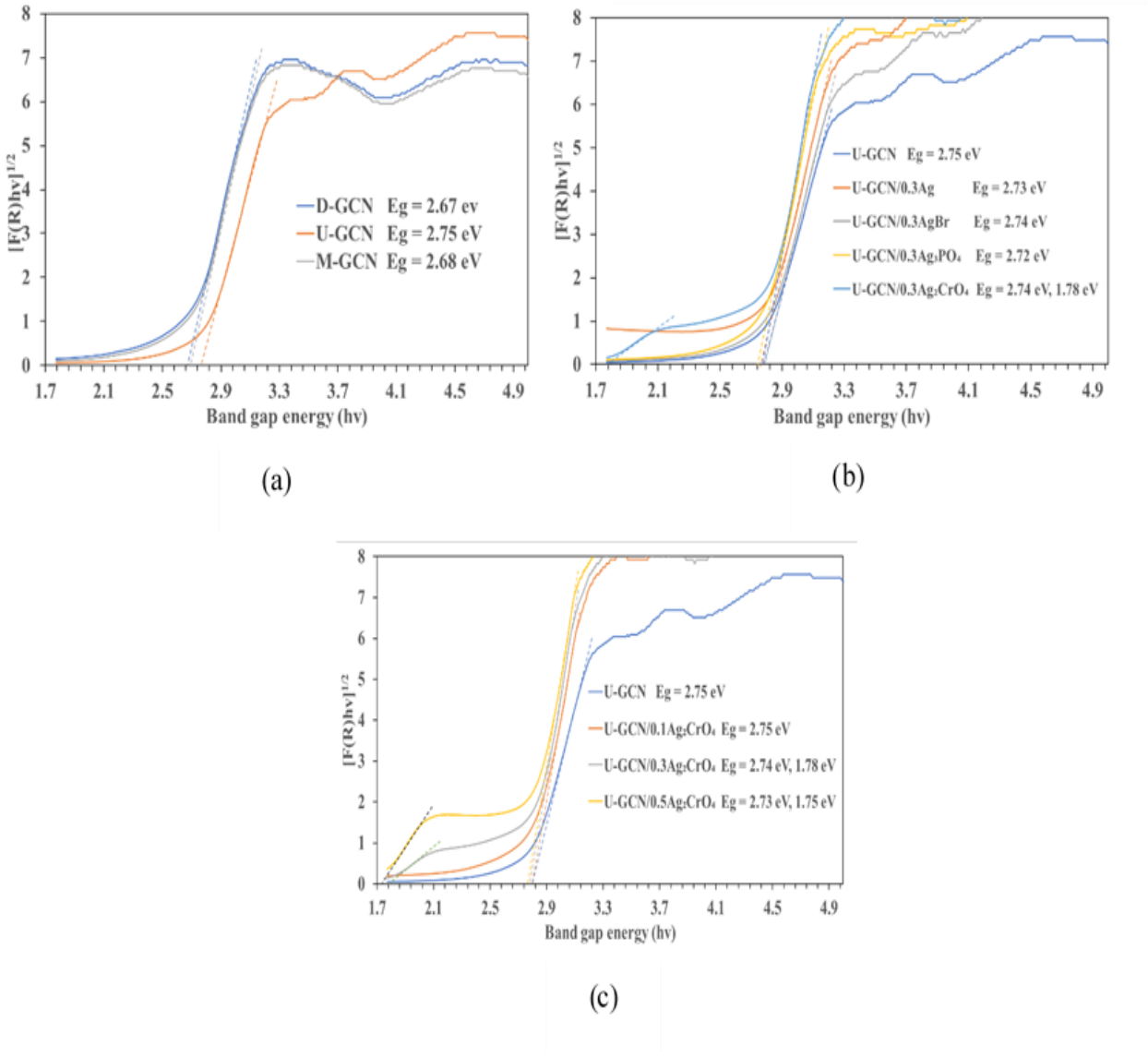

Figure S7. Bandgap energies of the photocatalysts: (a) GCNs derived from different precursors of dicyandiamide (D), urea (U), and melamine (M), (b) U-GCN/silver-based compounds, all in the same ratio of 1:0.3 and (c) U-GCN/xAg_2CrO_4 where x = 0.1, 0.3 and 0.5.

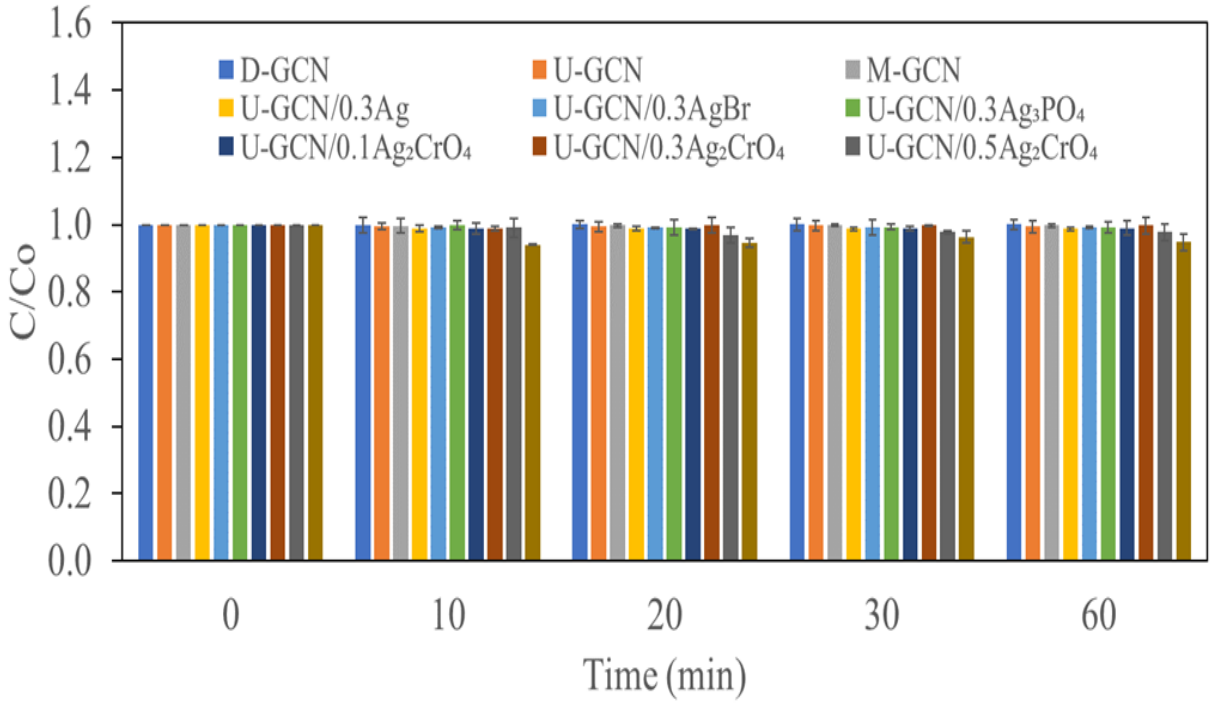

Figure S8. Adsorption performance of the synthesized photocatalysts on 4-CP in dark condition

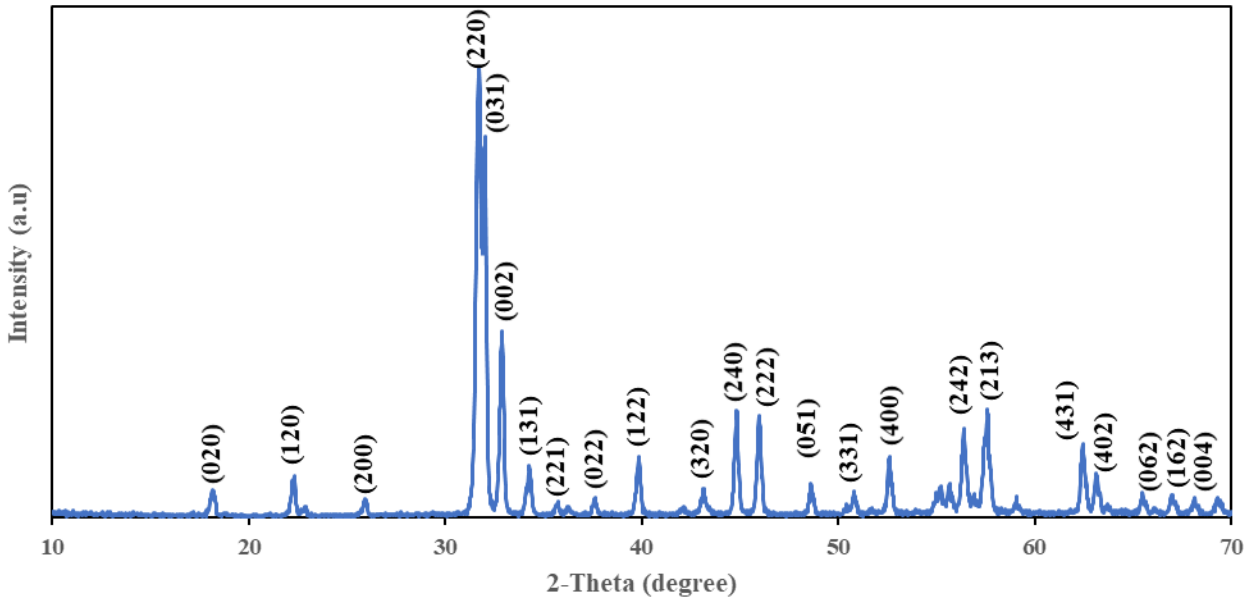

Figure S9. XRD pattern for Ag_2CrO_4

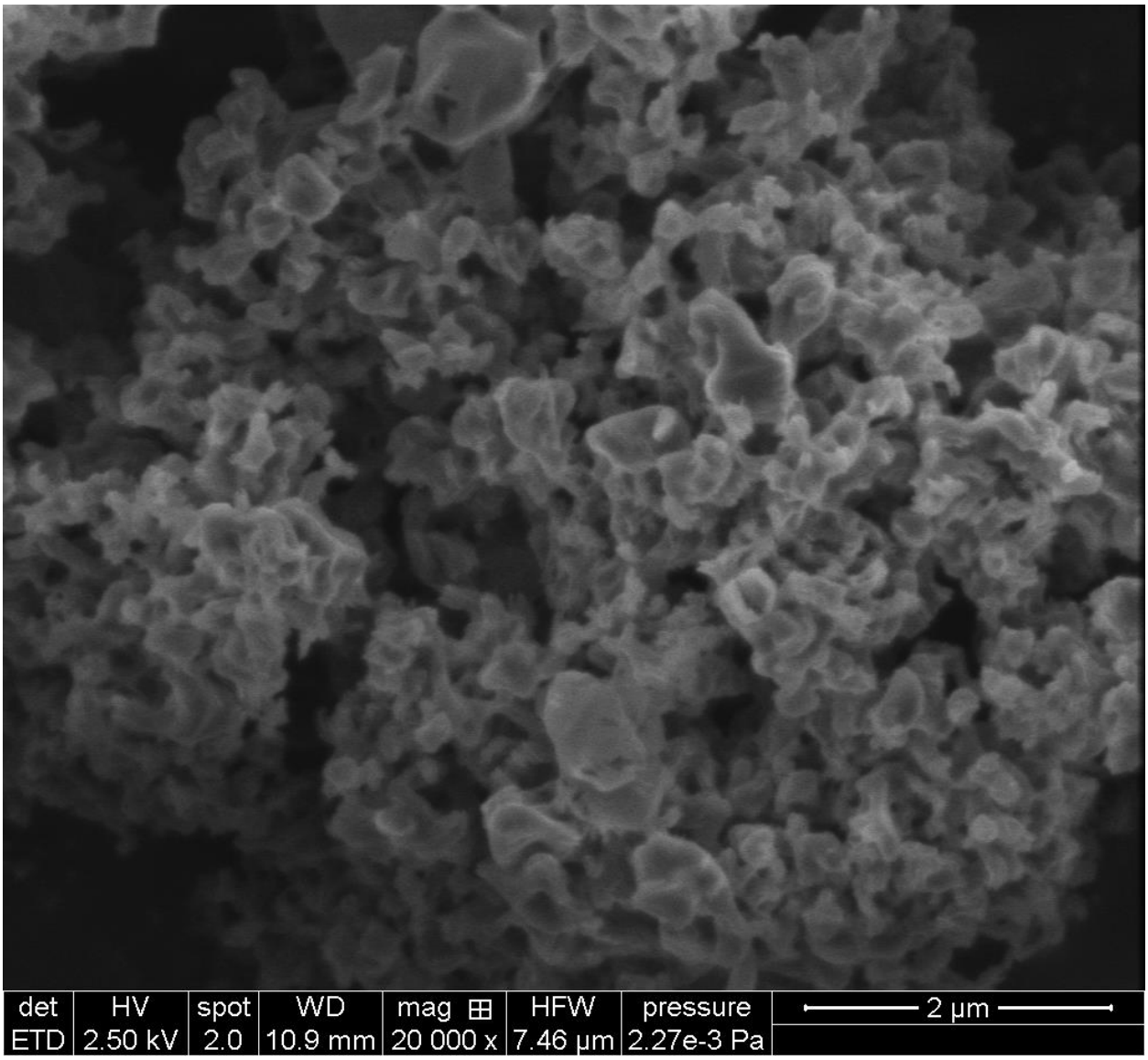

Figure S10. High-resolution SEM image of U-GCN/Ag_2CrO_4